

CRYSTALLIZATION OF THE LUNAR MAGMA OCEAN AND CONSEQUENCES FOR A CUMULATE MANTLE OVERTURN. K.A. Cone¹, S.M. Elardo², D. Hernández-Urbe³, W.A. Bohrsen¹, D.A. Manosalva², A.G. Distel⁴, F.J. Spera⁵ and R.M. Palin⁶; ¹Geology and Geological Engineering, Colorado School of Mines, CO, USA (kccone@mines.edu); ²Department of Geological Sciences, University of Florida, FL, USA (selardo@ufl.edu); ³Department of Earth and Environmental Sciences, University of Michigan, MI, USA; ⁴School of Earth and Space Exploration, Arizona State University, AZ, USA; ⁵Department of Earth Science, University of California, Santa Barbara, CA, USA; ⁶Department of Earth Sciences, University of Oxford, Oxford, UK.

Introduction: One of the most dynamic concepts in planetary evolution is a magma oceans as an inherent stage [1]. Our understanding of how a lunar magma ocean (LMO) may have cooled from a variably molten body to much of its current form is no less dynamic, evidenced by works exploring the effects of different bulk silicate compositions [2] magma ocean depths [2-4], heat piping [4], radiogenic heat [5,6], and end member cooling behavior (i.e. fractional vs. equilibrium crystallization [2, 7-9]).

The obvious consequence of an LMO is that it must eventually cool and solidify, forming an initial compositional and rheological structure. First-order characteristics of this initial form are primarily controlled though assumptions of bulk silicate Moon (BSM) composition, initial LMO depth, and cooling behavior. Published models, although varied in the above parameters, often produce similar characteristics for a bottom-up cooling of the LMO—an anorthosite flotation crust, late-stage Fe-enrichment of melt, formation of a dense sub-crustal ilmenite-bearing layer (IBL), and a progressively Mg-rich mantle with depth, are common. The density contrast between IBL and the underlying mantle is expected to force mantle mixing after the complete formation of the anorthositic flotation crust but possibly before full solidification of the remaining LMO. This mantle overturn [10,11] is commonly referred to as the cumulate mantle overturn (CMO) and likely involves complex multi-phase magma mixing/mingling, potentially along the entire depth of the LMO [12]. Earlier-formed high-Mg mafic phases may then be stirred up into the upper mantle where they imprint their deep mantle signatures. Therefore, the effects of mixing components between the interfacing IBL and mantle are controlled not only by mixing lengthscale but by phases predicted to exist at various depths from the initially modeled compositional structure.

We are in the process of creating multiple LMO fractional crystallization models to assess the potential consequences for post-CMO structures. Here we show preliminary results of the initial pre-CMO compositional structure predicted using forward phase equilibrium modeling of a single BSM composition and the effects of crystal settling. Changes in compositional

structure during the pre-to-post-CMO transition will later be determined using approaches that consider different degrees of magma mixing and/or mingling (i.e. homogenization) over varying depth.

Methods: The vertical sequence of stable phases formed from the bottom-up cooling of an LMO of Lunar Primitive Upper Mantle (LPUM) composition is predicted using Gibbs free energy minimizations via *Perple_X* [13]. Calculations were performed in the KNCFMASCTr system at ~1W buffer using appropriate solid solution models and a thermodynamic dataset suitable for peridotite compositions [14-16]. The slopes of cooling paths are varied, and a 1% volume of instantaneous trapped melt retained. In some cases, an adiabat is assumed to lie perfectly between the liquidus and solidus while in others the adiabat crosses the liquidus. The results of variably homogenizing the phases contained within the IBL and mantle are then assessed using Magma Chamber Simulator [17] and *Perple_X*.

Results and Discussion: A schematic of the initial compositional structure resulting from the fractional crystallization of an LMO of LPUM composition along a 50% crystal-50% melt path is shown in Fig. 1. This model *can produce* the formation of a ~44-km thick anorthosite crust (where plagioclase flotation begins at ~77% LMO solidification), underlain by a quartz-rich lens, then a secondary layer of plagioclase, *if* the cooling rate permits (i.e. cooling is slow). These results rest on the assumption that the instantaneous separation of dense phases from their immediate melt environment is efficient and complete in a constant 50/50 crystal/melt environment. Because density-driven crystal settling is modeled within confined vertical layers produced from a fractionally crystallizing LMO, too few layers produce too low a compositional resolution. We maintained ~30 layers, focusing on increased resolution of late-formed layers to better constrain the initial compositional characteristics of the IBL and upper mantle that define the initial P-T-X mixing conditions.

Interesting behaviors produced from this model (other than the formation of negatively buoyant plagioclase due to a progressively SiO₂-enriched melt environment) include density oscillations of late-formed phases (Fig. 2) that occur in part due to thickening of the

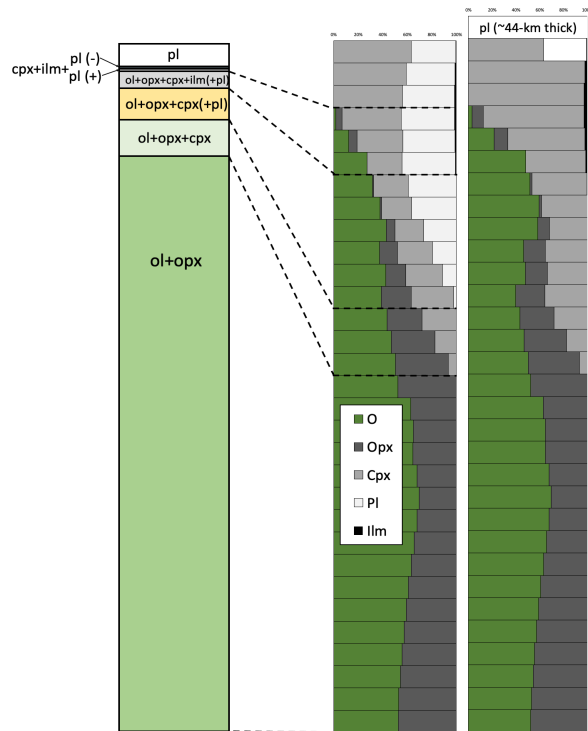


Figure 1. A schematic of the compositional layering of the Moon, before (center) and after (right) the sinking of dense phases from a fractionally crystallizing LMO along an adiabat that always lies perfectly between the liquidus and solidus. Cooling begins at a temperature halfway between the solidus and liquidus where opx and olivine co-precipitate. Layer thicknesses are not to scale, mineral modes are shown relative to 100% (center and right). From Cone et al. (in prep).

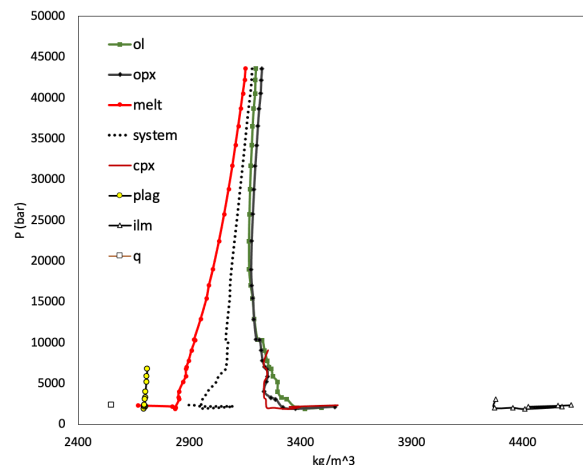


Figure 2. Evolving phase density profiles along a constant 50% melt path. Due in part to the pressure effects of a reversing cooling front and progressive Fe-enrichment, phases may display density inversions. Late-stage density oscillations occur primarily at $P < 0.5$ GPa.

anorthosite crust at its base—this forces a reversal in the direction of the cooling front while crystallization continues. Modal plagioclase and ilmenite both peak immediately before the formation of a quartz lens where plagioclase then sinks within that lens.

The timing of the CMO plays a key role in determining the components that mix and variably homogenize as well as the depth over which this mixing occurs in the lunar mantle [18]. We observe here that under the model's parameters, if an overturn event initiates before the LMO fully solidifies, then overturn may begin at ~60-km depth (defined by the first appearance of ilmenite), where the anorthosite crust is ~16-km thick, and ~90% of the LMO has solidified. To what extent ilmenite crystallization and sinking may impede efficient and complete flotation of co-crystallizing plagioclase remains poorly understood.

Our work aims to better understand the potential effects of CMO mixing, changes in P-T-X conditions along a vertical mixing profile in the lunar mantle, the resulting compositional structures, and how these structures may provide insight into the origin of the mare basalts.

References:

- [1] Schaefer and Elkins-Tanton (2018) *Phil. Trans. R. Soc. A*, 376, 20180109. [2] Elardo et al. (2011) *GCA*, 75, 3024-3045. [3] Elkins-Tanton et al. (2011) *EPSL*, 304, 326-336. [4] Maurice et al. (2020) *Sci. Adv.*, 6, eaba8949. [5] Tian et al. (2021) *Nature*, 600, 59-63. [6] Borg et al. (2004) *Nat.*, 432, 209-211. [7] Rapp and Draper (2018) *Meteorit. Planet. Sci.*, 53, 1432-1455. [8] Spera (1992) *GCA*, 56, 2253-2265. [9] Tonks and Melosh (1990) *LPI*, 151-174. [10] Snyder and Taylor (1992) *LPSC XXIII*, 1317-1318. [11] Hess and Parmentier. (1995) *EPSL*, 134, 501-514. [12] Zhao et al. (2019) *EPSL*, 511, 1-11. [13] Connolly (2005) *EPSL*, 236, 524-541. [14] Jennings and Holland (2015) *J. Pet.*, 56, 869-892. [15] Holland et al. (2018) *J. Pet.*, 59, 881-900. [16] White et al. (2000) *J. Metamorph. Geol.*, 18, 497-511. [17] Bohrsen et al. (2014) *J. Pet.*, 55, 1685-1717. [18] Boukaré et al. (2018) *EPSL*, 491, 216-225.